JOURNAL OF CATALYSIS 108, 323–333 (1987)

The Structure of Cu/SiO_2 Catalysts Prepared by the Ion-Exchange Technique

M. A. KOHLER,* H. E. CURRY-HYDE,* A. E. HUGHES,† B. A. SEXTON,†,[1] AND N. W. CANT*

*School of Chemistry, Macquarie University, North Ryde, New South Wales 2113, and †CSIRO Division of Materials Science, Locked Bag 33, Clayton, Victoria 3168, Australia

Received December 2, 1986; revised July 14, 1987

A series of Cu/SiO_2 catalysts prepared by the ion-exchange method and containing 2.1 to 9.5 wt% copper are characterised in detail by TEM, X-ray diffraction analysis, XPS, and TPR/TPO cycles. Two distinctly different copper species are identified, i.e., isolated copper atoms attached to two neighbouring silanol groups (ion-exchanged) representing 10–25% of the copper loading, and the remainder concentrated in numerous small copper particles (<6 nm, typically 1–3 nm diameter). In the calcined but unreduced samples, copper is present as both Cu(II) ions and copper oxide agglomerates of flat disc or hemispherical shape. Upon reduction in H_2 and at temperatures up to 673 K, the ion-exchanged species reduce to Cu(I) only and retain their isolated nature. The CuO particles reduce to metallic copper. During reduction very little particle migration and agglomeration is observed, which we attribute to an interaction between the particles and the Cu(I)-modified support. Whereas the TPR results do not clearly show sequential stages in the reduction of CuO particles, the TPO experiments reveal three clearly defined reoxidation peaks which give information on the relative surface-to-volume ratios of the copper particles on the different catalysts. We suggest that the low deactivation rate for this type of catalyst is related to a strong interaction between the small copper particles and the ion-exchanged Cu(I) present on the SiO_2 surface.

1. INTRODUCTION

Copper on silica catalysts prepared by the ion-exchange technique has certain advantages for some dehydrogenation, ester cleavage, and nitrile hydrolysis reactions (*1–4*). Thus Sodesawa (*1*), studying the dehydrogenation of methanol to methyl formate, found catalyst deactivation rates much lower for this type of preparation than for any other type of copper catalyst. Similar effects were observed for the reverse hydrogenolysis of methyl formate to methanol (*2*). With the ion-exchanged catalyst significant deactivation could be induced only by deliberate inclusion of more than 2% carbon monoxide in the feed (*2, 5*).

The preparation of these catalysts was first reported by Kobayashi *et al.* (*6*) but we have recently reported a much more detailed study (*7*). Several parameters such as copper concentration in the preparation solution, the solution's pH, the type of silica used, and the washing procedure were found to determine the copper content of the dried catalyst. In accordance with the propositions of Shimokawabe *et al.* (*8*), the results indicated two different mechanisms of copper deposition:

(1) Ion exchange of $[Cu(NH_3)_4]^{2+}$ ions with pairs of silanol groups on the silica surface to form an extremely well-dispersed network of single copper(II) diammine ions (or very small agglomerates) attached to the silica surface. The two remaining ammonia ligands are then replaced by water and, eventually, hydroxyl groups when the catalyst is washed.

[1] To whom correspondence should be addressed.

0021-9517/87 $3.00

(2) Precipitation of Cu(II) as copper hydroxide from the preparation solution inside the interstitial volumes during the washing procedure when the latter was carried out at pH $\leq$ 9.

The combination of the resulting two different types of copper on the catalyst may well be responsible for the unique behaviour of this catalyst type. It might also be the origin of the low reproducibility of copper surface areas determined by both Sodesawa (*1*) and ourselves (*7*) with a standard nitrous oxide decomposition technique (*9*).

In an attempt to clarify the structure and the properties of these catalysts, a number of techniques have been applied to a series of samples. Measurements by transmission electron microscopy (TEM), X-ray diffraction with line broadening analysis to confirm particle crystallinity and size, X-ray photoelectron spectroscopy (XPS), and temperature-programmed reduction (TPR) and oxidation (TPO) are presented. We present evidence to support the presence of two distinctly different copper species on the reduced catalysts. We also discuss the effects of calcination and different washing procedures on the surface phases.

2. EXPERIMENTAL

Four samples of Cu/SiO_2 containing from 2.1 to 9.5 wt% copper were prepared by the ion-exchange method described in detail elsewhere (*7*). Additional results were obtained on a fifth sample which was washed in small amounts of dilute ammonia solution at pH 9. As expected from earlier findings the resulting copper loading of 4.4 wt% indicated that substantial amounts of copper had been removed by the alkaline washing solution (*3, 7*). Results with the ammonia-washed sample are discussed separately from those with the water-washed catalysts, since some differences were found.

Temperature-programmed reductions (in hydrogen) and oxidation (in oxygen) were carried out in the apparatus described by Foger and Jaeger (*10*). Samples of 12 to 40 mg (depending on the copper loading) were flushed with nitrogen at 393 K for 1 h to remove any excess water and cooled to ambient temperature. A mixture of 3% hydrogen in nitrogen or 1.14% O_2 in helium was introduced at a flow of 20 ml/min and the temperature was ramped to 623 or 773 K, respectively, at 10 K/minute. Product water was removed with a zeolite trap cooled in dry ice and located before the thermal conductivity detector. The rate of hydrogen removal was followed as a function of temperature (and time), and the total hydrogen consumption was obtained by integration of the curve. The output signal was calibrated by injecting 1 ml of H_2 or O_2 and the measured consumption is believed accurate to $\pm 5\%$.

Transmission electron microscopy (TEM) was carried out on a JEOL 100 CX electron microscope at 100-keV accelerating voltage. X-ray diffraction measurements were made with a Siemens D-500 diffractometer employing Cu $K\alpha$ radiation and scanned at one degree per minute. XPS and X-ray-induced Auger measurements were made using a Vacuum Generators ESCALAB system fitted with an *in situ* reduction chamber. The Cu/SiO_2 samples were dispersed on a 1.3-cm^2 stainless steel holder. After being dried by evacuation to 10^{-8} Torr in the preparation chamber, samples could be reduced in H_2 and (subsequently) reoxidized in a 1% O_2/He mixture or pure nitrous oxide. Between treatments, samples were transferred to the main chamber where XPS and X-ray-induced Auger measurements were carried out using an Al $K\alpha$ (1486.6 eV) or Mg $K\alpha$ (1253.6 eV) source. Reduced copper catalysts were found to be very air-sensitive, and the use of an *in situ* reduction cell ensured that no surface oxidation influenced the results. Spectra were accumulated by signal averaging on a Tracor Northern TN 1710 MCA. Binding energies were referenced to the silicon 2*p* line determined to be 103.3 eV by calibration against the Au 4*f*7/2 binding

energy of 84.0 eV on gold-decorated silica. Data are reported as the modified Auger parameter (α') proposed by Wagner *et al.* (*11*) and modified by Gaarenstrom and Winograd (*12*), i.e., $\alpha' = \alpha + h\nu = BE_P + KE_A$, where $h\nu$ is the photon energy, BE_P is the binding energy of the photoelectron, and KE_A is the kinetic energy of the X-ray induced Auger line.

The surface copper-to-silicon atom ratio was obtained from the equation

$$\frac{Cu}{Si} = \frac{I\,(Cu\ 2p3/2)}{I\,(Si\ 2p)} \cdot \frac{S(Si)}{S(Cu)} \qquad (1)$$

where the relative sensitivity factors $S(Si) = 0.82$ and $S(Cu) = 22.2$ were taken from Scofield (*13*). This equation assumes that the mean free path ($\alpha\ KE^{0.5}$) and spectrometer transmission function ($\alpha\ KE^{-0.5}$) terms cancel. In the evaluation of the intensity measurements we are more concerned with changes in the surface Cu/Si ratios rather than their absolute values. It was felt that the accuracy of Eq. (1), ±20% was sufficient for the present study, and a more detailed analysis of intensities was not attempted.

3. RESULTS AND DISCUSSION

3.1. Size and Geometry of the Copper Particles

The Cu/SiO_2 samples had the usual blue-green colour of Cu(II) ions after being dried at 393 K. Reduction in hydrogen at 573 K gave a uniformly black material which on long standing in air assumed a dark green tinge. Reoxidation above 550 K resulted in a grey-blue material which returned to the starting blue-green on standing in air. Several techniques were focused on the problem of copper particle size determination. X-ray diffraction analysis was made on the fresh and reduced (but air-exposed) samples, but no diffraction peaks above background noise were observed for a 2θ range from 15 to 80°, indicating a crystallite size below 5 nm (assuming a spherical geometry) or below 10 nm (for raft-like crystallites).

Unreduced catalysts. A typical TEM result representing a low copper loading (2.1 wt%) in the fresh (calcined) state is given in Fig. 1a. No evidence of crystalline copper could be identified in samples of low copper content (≤4.1 wt%) either from the micrographs or by electron diffraction analysis, despite the estimated detection limit of 1.5 to 2.0 nm. A small number of crystals between 2 and 3.5 nm diameter were observed in the 5.9 wt% sample (Fig. 1b), which also showed distinct diffraction patterns. The crystals range from relatively flat discs to near hemispherical shapes and are distributed quite irregularly on the surface of the approximately spherical silica particles (average diameter 15 to 20 nm). A high catalyst loading (9.5 wt%) increased both the number and size (to 3 to 6 nm) of the dark CuO spots on the silica surface, as depicted in Fig. 1c. Given the limits of particle size detection (1.5–2 nm) and based on the hypothesis of ion-exchanged and precipitated copper outlined above, the observation of the larger species alone is not surprising. Identification of isolated atoms or small clusters is usually not possible from TEM measurements, except of those with very high atomic numbers where the contrast is greater than with copper.

Reduced catalysts. All samples were then fully reduced in hydrogen (at 573 K) and passivated in N_2O (at 363 K) before reanalysis by TEM. Very little evidence of isolated particles (up to about 4 nm diameter) was found in the 2.1 and 4.1 wt% samples. Despite some reports of high mobility of metallic copper in some impregnated catalysts, leading to significant particle aggregation during reduction at 573 K (*14, 15*), microscopic evidence for such particle migration and agglomeration was negligible (Fig. 1d, 2.1 wt% sample) in this study. This indicates a fairly strong attachment of the precipitated copper to the silica through at least one point. Such surface bonding may occur through defects in the

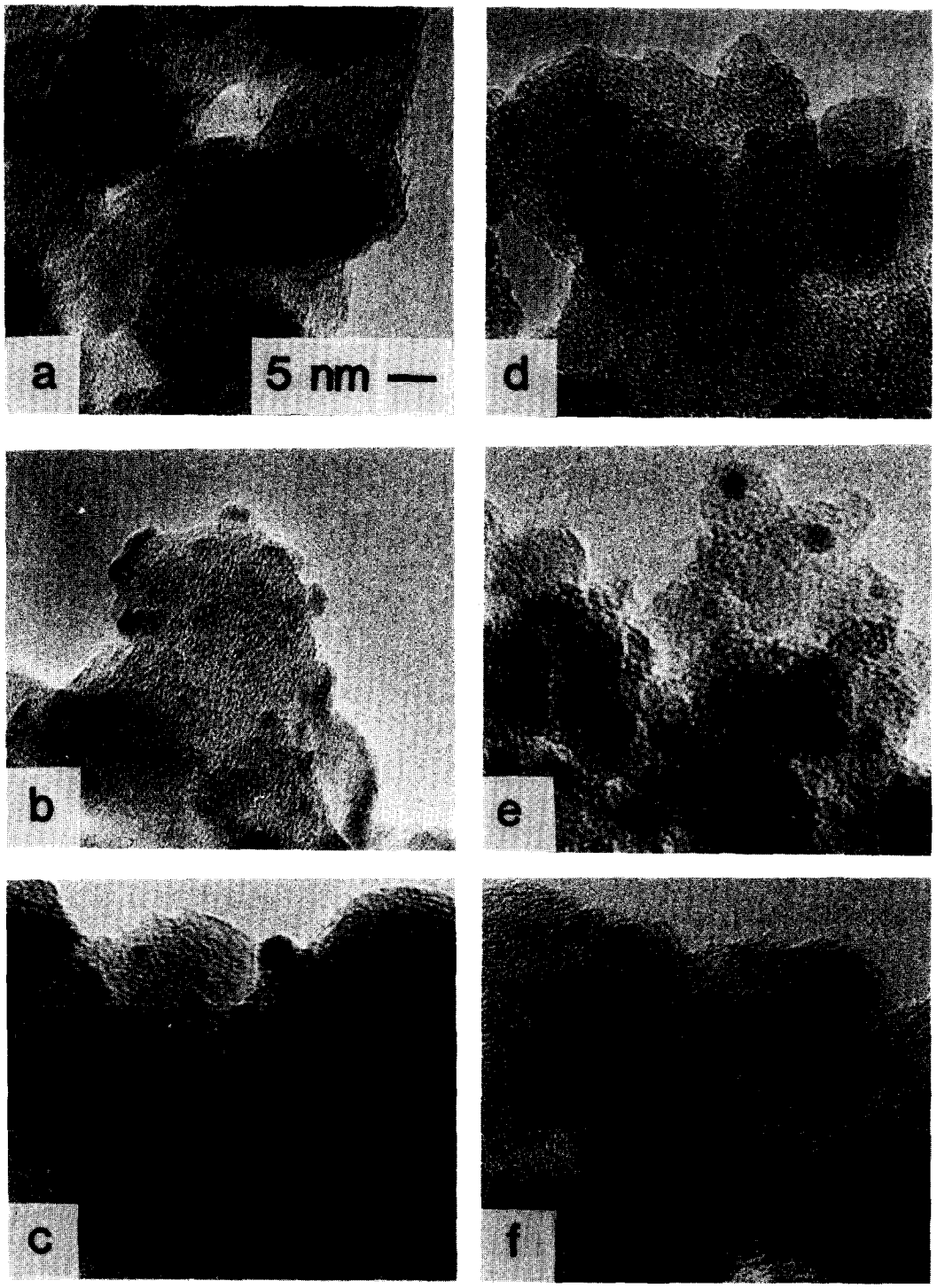

FIG. 1. Transmission electron micrographs of calcined Cu/SiO_2 catalysts containing different copper loadings. Samples (a) to (c) are unreduced and (d) to (f) are fully reduced and passivated in N_2O. Samples (a) and (d), 2.1 wt%; (b) and (e), 5.9 wt%; (c) and (f), 9.5 wt%.

silica surface or to ion-exchanged copper atoms, the latter possible from the mechanism proposed earlier (*7*). In both cases, after calcination, the precipitated copper oxide particles would be expected to agglomerate internally and to assume an approximately spherical shape during reduction (*14*), which would result in an apparent decrease of mean particle size. Effectively, both reduced higher loading samples reveal particles in about the same distribution frequency as before but of distinctly smaller average size (2 to 2.5 nm in the case of the 5.9 wt% sample, and 2 to 4 nm in the case of the 9.5 wt% sample as seen in Figs. 1e and 1f, respectively).

3.2. XPS Redox Sequences

XPS spectra of the Cu 2*p* 3/2 region and corresponding measurements of the X-ray-induced Cu L_3VV Auger line of a typical Cu/SiO_2 sample at various stages of its *reduction sequence* are shown in Figs. 2a and 2b, respectively. The XPS spectrum of the starting material (Fig. 2a(A)) has a characteristic shake-up satellite (at 943 eV) and a binding energy of 934.7 ± 0.2 eV. These features are representative of Cu(II) compounds and similar to the binding energy of Cu(II) ions in the channels of zeolites (*16*). The sum of the 2*p* 3/2 binding energy and the L_3VV Auger kinetic energy from Fig. 2b(A) results in an α' value of 1850 eV, which is similar to that of many Cu(II) compounds (*16*). Partial reduction of the surface copper phase was evident after treatment in hydrogen at 523 K. The shake-up satellite was progressively lost from the XPS spectrum accompanied by loss of the 934.7 eV Cu(II) line and appearance of an adjacent line at 932.5–932.0 eV, typical of either Cu(I) or Cu(0) (the two cannot be distinguished by examination of the Cu 2*p* 3/2 line alone). Separation of Cu(I) and Cu(0) can be made by reference to the L_3VV Auger line, however, and the results are shown in Figure 2b. The Cu(II) Auger line near 915.0 eV (Fig. 2b(A)) progressively disappears and splits into two components corresponding to Cu(I) at 914.2 ±

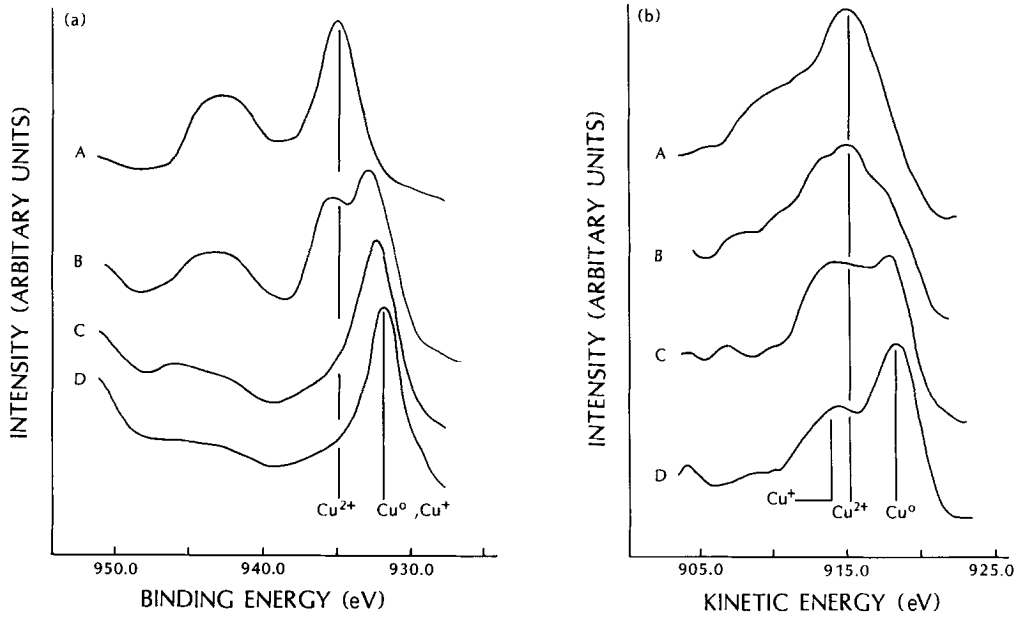

FIG. 2. (a) XPS Cu 2*p* 3/2 spectra of 4.4 wt% sample: A, unreduced calcined sample; B, reduced at 523 K for 15 min; C, reduced at 523 K for 30 min; D, reduced at 573 K for 10 min. (b) Cu L_3VV Auger spectra of 4.4 wt% sample: A, unreduced and calcined; B, reduced at 523 K for 15 min; C, reduced at 523 K for 30 min; D, reduced at 573 K for 10 min.

0.5 eV and Cu(0) at 918.3 ± 0.5 eV. As the reduction proceeds, signal growth is first concentrated in the Cu(I) component, then the Cu(0) peak becomes dominant in the latter stages. Finally, after hydrogen treatment at 573 K for 10 min, all evidence of residual Cu(II) species was lost. Any further reduction using longer exposure times or temperatures up to 650 K did not change the contributions from Cu(I) and Cu(0). The irreducible Cu(I) shoulder near 914 eV is a characteristic of this series of catalysts and we provide a more quantitative assessment of the peak later in this section. A fresh sample was then reduced at 573 K for 30 min and oxidised in 1% O_2/He at increasing temperatures. Starting from the reduced state, the oxidation increased gradually until after oxidation at 523 K for 5 min the Auger spectra resembled that of the starting material.

More detailed information can be obtained when both kinetic and binding energies of the spectroscopic results are analysed in a 2-D chemical state plot (*11, 12*) for various reduction/oxidation cycles as shown in Fig. 3. Known zones for copper metal and Cu(I) and Cu(II) compounds are represented by shaded areas, with four of the catalysts plotted as points 1 to 4 with increasing loading from 2.1 to 9.5 wt% respectively. The results fall into three zones, A, B and C. The unreduced catalysts in group A consist primarily of Cu(II) species. The low modified Auger parameters (α' values) of these Cu(II) species relative to those of normal Cu(II) compounds reflect the small CuO particle sizes as seen previously in the TEM results. Low α' values result from reduced coordination around the atoms (*16, 17*) and usually decrease with increasing dispersion of a compound. After reduction, two states are identified, a Cu(I) state (group B) and a metallic copper state (group C). Separation of the two reduced phases can be made only via the Auger L_3VV line since they have identical Cu 2*p* binding energies.

Two observations are important in Fig. 3.

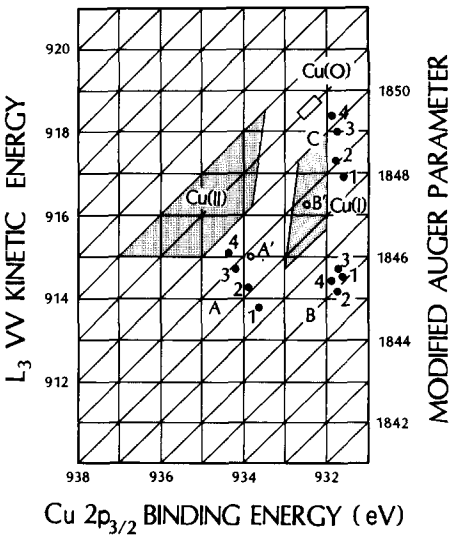

FIG. 3. 2-D chemical state plot of the reduction behaviour of a series of Cu/SiO_2 catalysts at various copper loadings. Group A represents the unreduced samples. Groups B and C, representing finely dispersed Cu(I) and Cu(0), respectively, are obtained upon reduction. Position B′ corresponds to the sample oxidized in 1% O_2/He at 173 to 428 K; A′ corresponds to the further oxidation at temperatures up to 773 K. Sample loadings: 1, 2.1 wt%; 2, 4.1 wt%; 3, 5.9 wt%; 4, 9.5 wt%.

The unreduced catalyst has substantial amounts of a CuO phase which does not completely reduce to metallic copper, and the irreducible Cu(I) state is present on all of the reduced catalysts, independent of loading. Second, as the copper loading decreases, the α' values of the CuO and Cu metal particles also decrease, which is consistent with a decrease in the average particle size (*16, 17*). The Cu(I) phase α' value, however, is independent of the loading, indicating a similar chemical state and dispersion of this phase on all catalysts. The α' value of 1846 ± 0.5 eV for the Cu(I) state is almost 2–3 V lower than that of normal Cu(I) compounds and consistent with an atomically dispersed phase as seen previously for Cu(I) in Y zeolites (*16*). When the catalysts were reoxidised in 1% O_2/He at up to 428 K the point B′ in Fig. 3 was obtained, consistent with an oxidation of the particles to Cu(I). Further oxidation at

773 K resulted in point A′, which indicated further oxidation to Cu(II), similar to the original starting material.

The two reduced phases, Cu metal and Cu(I), were separated by a curve subtraction procedure in the L_3VV Auger line, as shown in Fig. 4. A copper metal line shape (dashed curve in Fig. 4) was established from a fully reduced (728 K in flowing H_2 (*18*)) copper chromite (Harshaw 0203) sample. Subtraction of this line shape from the reduced Cu/SiO_2 spectra revealed the Cu(I) fraction near 914.5 eV. On the basis of the results in Fig. 4, we therefore propose a model of the reduced catalyst surface which incorporates copper metal particles of a size dependent on the loading dispersed on a network of Cu(I) atoms bound strongly to the silica support:

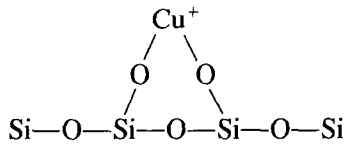

It is most likely that the source of the Cu(I) arises from the ion-exchanged copper attached to the silica as single atoms (*7, 19–21*). Precipitated $Cu(OH)_2$ in the interstitial volumes at pH <11 can account for the copper particles. We suggest that a high activation barrier toward breaking of Cu–O–Si bonds is responsible for the lack of reduction of the ion-exchanged phase, whereas CuO particles derived from the $Cu(OH)_2$ precursor would be easily reduced, as observed. The similar modified Auger parameters for Cu(I) on all the catalysts are consistent with a single highly dispersed phase, whereas the variation in the α' values for CuO and Cu particles can be explained by variation in particle size as outlined earlier.

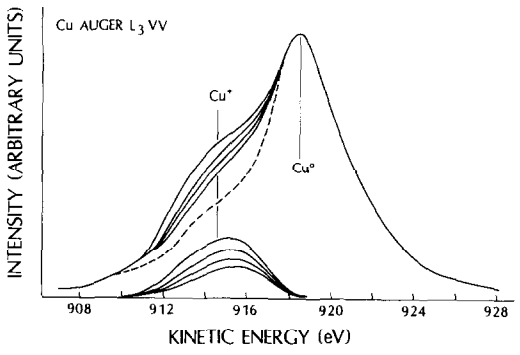

FIG. 4. Cu(I) loading dependence. The Auger line for reduced (723 K for 30 min in 20% H_2/Ar) Cu chromite (dashed line) is used as a standard to subtract out the Cu(0) component of each catalyst. From top to bottom the Cu loadings are 2.1, 4.1, 5.9, and 9.5 wt%. The spectra have been arbitrarily shifted along the B.E. scale to align the Cu(0) components.

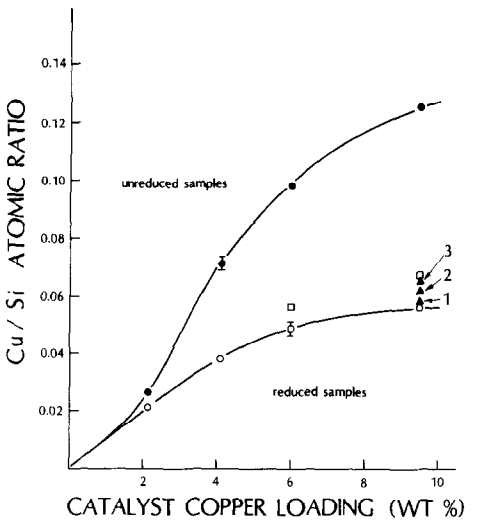

FIG. 5. Reduction dependence of Cu/Si atomic ratios (Eq. (1)) of calcined catalysts: ●, unreduced; ○, reduced; ▲, oxidized in N_2O at 363 K (1), 398 K (2), and 438 K (3); □, fully oxidized in 1% O_2/He at up to 773 K.

3.3. Cu/Si Atomic Ratio from XPS Measurements

In Fig. 5, we measured the surface Cu/Si ratios for the range of catalysts, both before and after reduction and after reoxidation. The surface Cu/Si ratio is sensitive to the dispersion of the copper phases since changes in particle morphology affect the escaping electron intensity, especially when the particle size becomes comparable to the mean free path.

For the unreduced samples, a nonlinear curve of Cu/Si ratio versus loading is found, with the ratio levelling off at higher load-

ings. After reduction, a decrease of a factor of almost two is found for loadings exceeding 4 wt% with a much smaller decrease for the 2.1 wt% sample. The general shape of the two curves can be explained by a model in which the average particle size begins to exceed the mean free path of the copper 2*p* electron (~1.5 nm) at high loadings. This assumes that the density of particles does not change significantly but that the size increases with higher loadings. For the 9.5 wt% catalyst, the estimated particle size was 2–4 nm, which is larger than the mean free path.

The decrease in intensity after reduction is more difficult to explain since only small differences were found in the average particle size before and after reduction from TEM measurements. The most plausible explanation is the presence of rafts or sheets of precipitated copper on the silica support in the calcined phase which escaped detection in the TEM micrographs. After reduction, such material could agglomerate to form extra spherical copper particles, exposing the silica surface and increasing the Cu/Si ratio by virtue of the reduced attenuation of the Si 2*p* line. That this agglomeration process is irreversible can be seen from the reoxidation experimental points in Fig. 5. Oxidation of the catalysts in either 1% O_2/He or N_2O produced only a slight increase in the Cu/Si ratio, indicating little redispersion of the oxidized copper. That is, no significant recoating of the silica support by raft-like deposits had occurred.

Calculation of the expected Cu/Si ratio (*22*), based on the copper loading and the silica surface area, indicates agreement with the extrapolated curves at loadings below 2 wt% where the particle size is less than the mean free path.

3.4. Temperature-Programmed Reduction

An initial TPR of a fresh, calcined Cu/SiO_2 was always characterized by a single and sharp consumption peak (width approximately 40 K) with a maximum rate at 505 K. Second (and subsequent) reductions commenced at the lower temperature of 393 K and were complete at 513 K. They showed a maximum rate at 464 ± 5 K and a shoulder at 476 ± 5 K. On the basis of experimental and theoretical (from Cu content) hydrogen consumption it was then possible to calculate the Cu(I) fractions of the reduced catalysts, which are shown in Table 1. A good agreement of the results with those obtained from integrating the Auger L_3VV peaks was found. Subsequent reductions (after intermediate TPO as described below) always consumed less (but constant) hydrogen than the first reduction, which clearly indicates that the reoxidation to Cu(II) was incomplete. The Cu(I) fractions in the reduced catalyst were recalculated on the basis of this difference, giving results similar to those of the first TPR. When experimental error was taken into account, approximately 10 to 15% of isolated Cu(I) atoms were estimated to have reoxidized after reoxidation at 773 K. This conclusion is supported by theoretical and experimental findings for the oxidation states of copper on alumina (*19*), indicating a stability analogous to that of the Cu^+ state on the present silica support.

3.5. Temperature-Programmed Oxidation

Figure 6 displays oxygen uptake traces for freshly reduced samples at tempera-

TABLE 1

The Cu(I) Fractions on Reduced Catalysts Determined by a Curve-Fitting Separation of the Auger L_3VV Line (Fig. 4) and the First and Subsequent TPR Analyses

Catalyst loading (wt%)	Cu(I), Auger	Cu(I), TPR1	Cu(I), TPR2
2.1	0.20 ± 0.02	0.23 ± 0.01	0.20 ± 0.02
4.1	0.15 ± 0.02	0.18 ± 0.01	0.16 ± 0.02
5.9	0.12 ± 0.01	0.15 ± 0.01	0.13 ± 0.01
5.9[a]			0.12 ± 0.01
9.5	0.10 ± 0.01	0.13 ± 0.01	0.12 ± 0.01

[a] After further reoxidation (TPO) at up to 773 K.

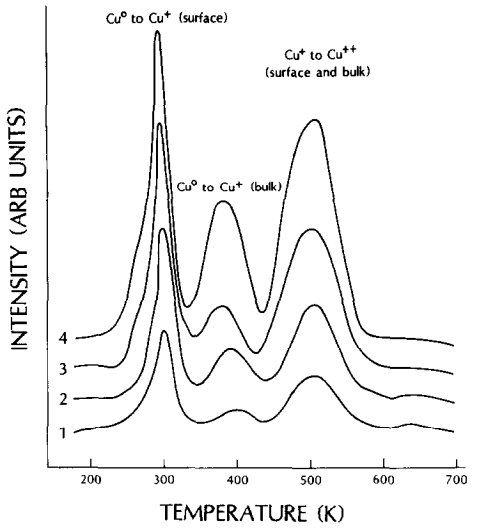

FIG. 6. Temperature-programmed oxidation of calcined Cu/SiO_2 catalysts in 1.14% O_2/He (20 ml/min) between 173 and 700 K. Sample copper loadings: 1, 2.1 wt%; 2, 4.1 wt%; 3, 5.9 wt%; 4, 9.5 wt%.

tures between 173 and 700 K (no significant further uptake was detected up to 773 K). Three major peaks can be identified for the four catalysts with maximum oxygen consumptions at 295 ± 2 K, 378 to 397 K (depending on the catalyst loading), and 493 ± 2 K. A fourth peak around 620 K is very small and broad and is clearly visible only in samples of low copper content. The detailed analysis of the oxygen uptakes in Table 2 reveals that the sum of peaks 1 and 2 equals peak 3 (within experimental error), although the ratio of 1 to 2 decreases significantly with copper loading. In order to identify the oxidation states contributing to the different peaks, TPO's of the 5.9 wt% sample were rerun and stopped at different stages of reoxidation, transferred to the ESCALAB, and analyzed by XPS. After oxidation to 320 K, a significant increase in the Cu(I) fraction (ca. 60%) was detected from the Auger line, the remainder being Cu(0) with the latter disappearing almost completely as the oxidation progressed to 430 K. Completing the oxidation at 773 K resulted in a major fraction of Cu(II) and a minor contribution from Cu(I). The three main TPO peaks are therefore assigned as follows:

(1) Surface oxidation of precipitated Cu(0) clusters to Cu(I).
(2) Bulk oxidation of these particles to Cu(I).
(3) Surface plus bulk oxidation of the same clusters to Cu(II).

The asymmetry of the first peak is probably related to the copper particle size distribution and/or the accessibility of the surface atoms to oxygen (*20*). On the assumptions of 1.46×10^{19} Cu atoms/m^2 of surface (*9*) and single-layer oxidation, it was then possible to calculate the corresponding Cu(0)

TABLE 2

Copper Oxidation Calculated from Oxygen Uptakes in the Three Major TPO Peaks (Figure 6), and the Corresponding Surface Areas and Mean Copper Particle Size Calculated on the Assumption of Monolayer Oxidation

Catalyst loading		Peak 1 Cu^0 to Cu^+ surface (mol Cu/g) ($\times 10^4$)	Peak 2 Cu^0 to Cu^+ bulk (mol Cu/g) ($\times 10^4$)	Peak 3 Cu^+ to Cu^{2+} bulk and surface (mol Cu/g) ($\times 10^4$)	Cu surface area (m^2/g)	Particle diameter (nm)
(wt%)	(mol Cu/g) ($\times 10^4$)					
2.1	3.31	2.37	0.89	3.22	9.8	1.4
4.1	6.46	4.51	1.83	6.05	18.6	1.5
5.9	9.29	6.25	2.66	9.22	25.7	1.6
9.5	15.0	8.13	3.99	13.1	33.4	2.0
5.9[a]	9.29	5.60	3.45	9.42	23.1	1.9

[a] After further rereduction (TPR) at up to 623 K.

surface areas of the catalysts and the mean copper particle size (Table 2). For any catalyst of this series, the metallic copper surface areas inferred are 1.8 ± 0.1 times those found by the modified nitrous oxide decomposition method (*7*) on the same samples. The first step of the oxidation is therefore concluded to comprise slightly less than two copper layers, which is reasonable with respect to the oxidation mechanism proposed in the literature (*23, 24*). A similar conclusion is reached when crystallite size calculated from the oxygen uptake (Table 2) is compared with those found by TEM (Figs. 1e and f). If the N_2O results are assumed to be correct, crystallite sizes very similar to those identified by TEM are found. The size of the metallic copper particles should also be related by the area ratio of peaks 1 and 2 (near-surface and volume oxidation, respectively). It is clear from Fig. 6 and Table 2 that copper dispersion increases significantly with decreasing catalyst loading. In accordance with XPS results, no copper particles are expected to be larger than the detection limit of TEM at loadings below approximately 4 wt%, even when the conservative copper surface measurements are adopted.

The Cu(I) fraction in the reduced samples cannot be accurately determined from the TPO analysis. It is clear, however, that in any sample the experimental oxygen uptake is smaller than the theoretical value based on the total copper content (Table 2). Furthermore, given its size, shape, and location, in comparison with those given by Baiker *et al.* (*25*), the remaining peak around 620 K most likely represents the small fraction of isolated Cu(I) oxidizing to a Cu(II) state. We also investigated the effect of reduction–oxidation cycles on the TPO spectra. Subsequent TPO's always showed a considerable change in relative area of the two peaks corresponding to surface and bulk oxidation of Cu to Cu^+ but little effect on the size of the peak due to the conversion of Cu^+ to Cu^{2+}. The copper surface area must therefore decrease somewhat as a result of the first oxidation.

3.6. The Effect of Washing in Ammonia (pH 9)

It is interesting to note at this stage the results collected on a catalyst (4.4 wt%) subjected to washing at pH 9 prior to calcination. When the same analyses as before were followed, an average Cu(I) fraction of 0.20 was found (TPR, Auger), which is somewhat higher than expected from the sequence in Table 1. Correspondingly, a Cu/Si atomic ratio of 0.059 was evaluated on the unreduced sample which dropped to 0.038 during reduction. A comparison with the results in Fig. 4 suggests a substantially smaller fraction of the precipitated copper species in this sample. These results suggest that copper was concentrated in the ion-exchanged species (compared to washing at pH 7) most probably as a result of the higher solubility of precipitated Cu^{2+} during the washing procedure (*7*). A thorough washing in a large excess of distilled water and avoiding a high-pH solution, followed by calcination at up to 773 K, seem therefore necessary conditions for high Cu(0) contents in the catalysts.

4. CONCLUSIONS

The structure and distribution of copper on a silica support prepared by the ion-exchange method have been clarified by a comparison the results of a number of different characterization techniques. Two distinct species of copper with considerably different structural and possibly reactive properties or catalytic behaviour are identified:

(1) Isolated copper ions attached to two neighbouring silanol groups and building up a copper network on the silica surface. The saturation of the silanol groups is approximately 60% (*7*) and little affected by washing at pH ≤ 9. This copper species reduces to Cu^+ but not to metallic copper and could

well be catalytically inactive in a number of applications.

(2) Numerous copper hydroxide particles precipitated from the preparation solution in the support interstices during the washing procedure. After calcination to CuO, the mean particle size varies from about 1.5 nm (at low copper content) to 3–6 nm (at high loadings) with the particles being of flat disc or hemispherical shape and irregularly distributed on the silica surface. Upon reduction, this fraction of the copper reduces to the metallic state with internal agglomeration of the particles to approach a spherical shape.

The ratio of Cu(0) to Cu(I) in the reduced state is therefore governed by the ratio of precipitated to ion-exchanged species. High concentrations in the preparation solution, washing in neutral solution, and lower silica surface areas (*7*) favour higher copper metal fractions, but the active surface area is expected to plateau at about 10 wt% catalyst loading (Table 2). The relatively stable and high activity per copper weight of these catalysts observed in a number of applications (*2–5*) can therefore be attributed to extremely small copper particles which are separated from each other by a multiple of their size. Additionally, a metal-to-support interaction appears to restrict particle movement even at fairly high temperatures in hydrogen or oxygen and helps prevent thermal sintering of the copper surface.

ACKNOWLEDGMENTS

The authors thank A. Agarwal and J. C. Lee for their assistance in catalyst preparation, H. K. Jaeger for permission to publish the TEM micrographs, K. Foger for assistance with the TPR and TPO experiments, and D. L. Trimm and M. S. Wainwright for useful discussions. Financial support by the Australian Research Grants Scheme and a joint CSIRO–Macquarie University grant is gratefully acknowledged.

REFERENCES

1. Sodesawa, T., *React. Kinet. Catal. Lett.* **24,** 259 (1984).
2. Monti, D. M., Wainwright, M. S., Trimm, D. L., and Cant, N. W., *Ind. Eng. Chem. Prod. Res. Dev.* **24,** 397 (1985).
3. Tonner, S. P., Trimm, D. L., Wainwright, M. S., and Cant, N. W., *Ind. Eng. Chem. Prod. Res. Dev.* **23,** 384 (1984).
4. Kohler, M. A., Lee, J. C., Wainwright, M. S., Trimm, D. L., and Cant, N. W., *Appl. Catal.*, to appear.
5. Monti, D. M., Cant, N. W., Trimm, D. L., and Wainwright, M. S., *J. Catal.* **100,** 17 (1986).
6. Kobayashi, H., Takegawa, N., Minochi, C., and Takahashi, K., *Chem. Lett.*, 1197 (1980).
7. Kohler, M. A., Lee, J. C., Cant, N. W., Wainwright, M. S., and Trimm, D. L., *Appl. Catal.* **31,** 309 (1987).
8. Shimokawabe, M., Takegawa, N., and Kobayashi, H., *Appl. Catal.* **2,** 379 (1982).
9. Evans, J. W., Wainwright, M. S., Bridgewater, A. J., and Young, D. J., *Appl. Catal.* **7,** 75 (1983).
10. Foger, K., and Jaeger, H. K., *J. Catal.* **67,** 252 (1981).
11. Wagner, C. D., Galeand, L. H., and Raymond, R. H., *Anal. Chem.* **51,** 466 (1979).
12. Gaarenstroom, S. W., and Winograd, N., *J. Chem. Phys.* **67,** 3500 (1977).
13. Scofield, J. H., *J. Electron Spectrosc. Relat. Phenom.* **8,** 129 (1976).
14. Jacobs, P. A., Jaeger, N., Jira, P., and Schultz-Ekloff, G. (Eds.), "Metal Microstructures in Zeolites, Studies in Surface Science and Catalysis," Vol. 12. Elsevier, Amsterdam, 1982.
15. Texter, J., Strome, D. H., Hermann, R. G., and Klier, K., *J. Phys. Chem.* **81,** 333 (1977).
16. Sexton, B. A., Smith, T. D., and Sanders, J. V., *J. Electron Spectrosc. Relat. Phenom.* **35,** 27 (1985).
17. Kowalczyk, S. P., Ley, L., McFeely, F. R., Pollak, R. A., and Shirley, D. E., *Phys. Rev. Sect. B* **9,** 381 (1974).
18. Evans, J. W., Casey, P. S., Wainwright, M. S., Trimm, D. L., and Cant, N. W., *Appl. Catal.* **7,** 31 (1983).
19. Lo Jacono, M., Cimino, A., and Inversi, M., *J. Catal.* **76,** 320 (1982).
20. Takezawa, N., Kobayashi, H., Kamegai, Y., and Shimokawabe, M., *Appl. Catal.* **3,** 381 (1982).
21. Peri, J. B., *J. Catal.* **41,** 227 (1976).
22. Kerkhof, F. P. J. M., and Moulijn, J. A., *J. Phys. Chem.* **83,** 1612 (1979).
23. Habraken, F. H., Mestos, C. M., and Bootsma, G. A., *Surf. Sci.* **97,** 204 (1980).
24. Giamello, E., Fubini, B., Lauro, P., and Bossi, A., *J. Catal.* **87,** 443 (1984).
25. Baiker, A., Monti, D., and Wokaun, A., *Appl. Catal.* **23,** 425 (1986).